



ELSEVIER

Magnetic resonance microscopy: recent advances and applications

J Michael Tyszka, Scott E Fraser and Russell E Jacobs

Magnetic resonance microscopy is receiving increased attention as more researchers in the biological sciences are turning to non-invasive imaging to characterize development, perturbations, phenotypes and pathologies in model organisms ranging from amphibian embryos to adult rodents and even plants. The limits of spatial resolution are being explored as hardware improvements address the need for increased sensitivity. Recent developments include *in vivo* cell tracking, restricted diffusion imaging, functional magnetic resonance microscopy and three-dimensional mouse atlases. Important applications are also being developed outside biology in the fields of fluid mechanics, geology and chemistry.

Addresses

Biological Imaging Center, Division of Biology, California Institute of Technology, 2Q Broad 114-96, 1200 East California Boulevard, Pasadena, CA 91125, USA

Corresponding author: Tyszka, J Michael (jmt@caltech.edu)

Current Opinion in Biotechnology 2005, 16:93–99

This review comes from a themed issue on
Analytical biotechnology
Edited by Keith Wood and Dieter Klaubert

Available online 8th December 2004

0958-1669/\$ – see front matter
© 2005 Elsevier Ltd. All rights reserved.

DOI 10.1016/j.copbio.2004.11.004

Abbreviations

BOLD	blood oxygenation level dependent
DSI	diffusion spectrum imaging
DTI	diffusion tensor imaging
fMRI	functional magnetic resonance imaging
MRI	magnetic resonance imaging
MRM	magnetic resonance microscopy
NMR	nuclear magnetic resonance

Introduction

Magnetic resonance imaging (MRI) is now well established as the premier non-invasive imaging modality for the central nervous system in humans. Magnetic resonance microscopy (MRM) has also seen a great deal of parallel development, with many of the advances in clinical MRI reapplied at smaller scales. The boundary between MRI and MRM is relatively vague, with imaging at spatial resolutions in the order of 100 μm and smaller typically considered to be microscopy (Figure 1). By this definition, some high-resolution MRI in humans qualifies

as microscopy, but we will limit this review to organisms and sample sizes less than a few centimeters across.

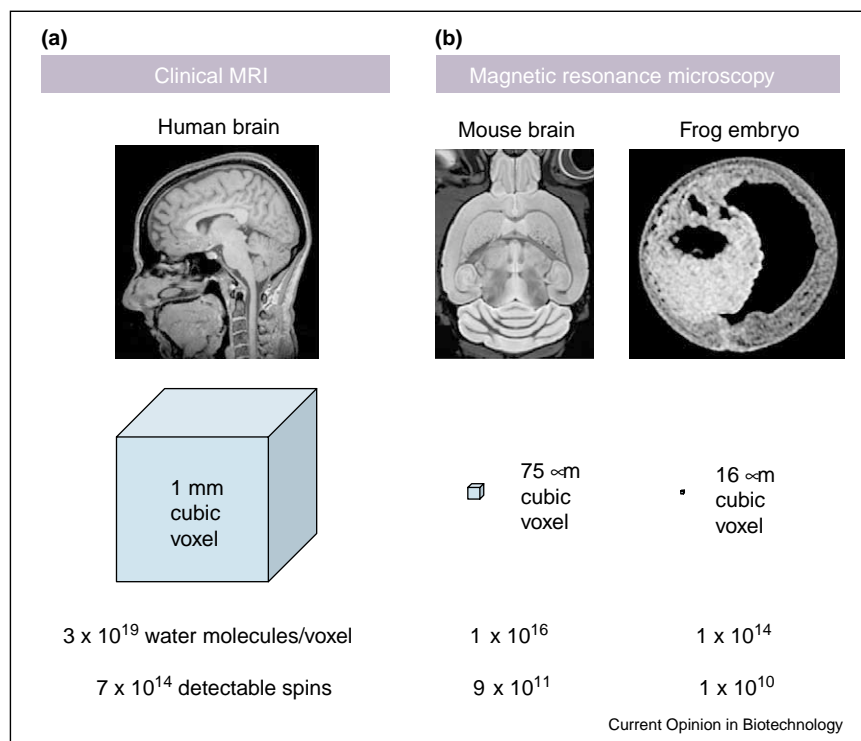
MRI exploits the nuclear magnetism exhibited by certain nuclei such as ^1H , ^{19}F , ^{13}C and ^{31}P . By far the most common nucleus visualized by MRI is ^1H , with close to 100% natural abundance and high magnetic resonance sensitivity. The composition of most biological tissue is dominated by liquid water, and it is the difference in water environment between different tissues that MRI visualizes so effectively.

Both MRI and nuclear magnetic resonance (NMR) rely on the presence of a strong magnetic field to polarize the bulk nuclear magnetism in an object. A pulse of radio-frequency radiation perturbs the nuclear magnetization and allows a signal to be induced in a receiver coil. The Larmor relation ($\omega = \gamma B$) between NMR precession frequency, ω , gyromagnetic ratio, γ , and magnetic field strength, B , is exploited to spatially resolve the nuclear magnetism within a sample. Pulsed magnetic field gradients are combined with radiofrequency pulsing to encode spatial position in the frequency and phase of the received signal, allowing reconstruction of a magnetic resonance image. See books by Haacke *et al.* [1] and Callaghan [2] amongst others for detailed reviews of the principles of MRI.

Perhaps the most important issue for MRM is the fundamental limit to spatial resolution. Various authors have estimated the limit to be in the order of 1 μm for liquid water at room or physiological temperatures based on arguments of molecular diffusion, T_2 relaxation (an NMR signal decay mechanism), microscopic field inhomogeneity and the sensitivity of the NMR experiment to diminishing numbers of nuclear spins [2]. MRM images are only rarely acquired at isotropic spatial resolutions less than 10 μm . In practice, the spatial resolution is limited by sensitivity factors, specifically the signal-to-noise ratio achievable in a given time. For *in vivo* imaging, the total imaging time is constrained by physiological tolerance and anesthetic constraints. For *in vitro* and *ex vivo* samples, more mundane constraints, such as equipment schedules and system stability, limit practical imaging times.

There is a general consensus within the MRM community that high-resolution imaging with spatial resolution of less than 100 μm benefits from the use of high-field magnets, with field strengths greater than 3 Tesla. The primary benefit to MRM is an increase in the nuclear

Figure 1



Comparison of (a) clinical MRI with (b) MRM. The key difference is in the spatial resolution, implied by the nominal volume element (voxel) dimension. The total number of nuclear spins available for imaging also decreases with voxel volume, but can be partly restored by increased magnetic field strength, which increases the fraction of spins that contribute to the MRM signal. The estimates of detectable spins in this figure are based on 3 Tesla and 37 °C for human brain, 9.4 Tesla and 37 °C for mouse brain and 11.7 Tesla and 15 °C for frog (*Xenopus laevis*) embryos. The number of detectable spins per voxel drops by almost five orders of magnitude between human brain MRI and frog embryo MRM, requiring significant hardware sensitivity increases to maintain signal-to-noise ratio.

polarization fraction contributing to the image; however, other factors, such as a general increase in the T_1 relaxation time, decrease in T_2 and increased susceptibility-based field inhomogeneity, are all confounding factors at high field strengths.

There is less debate surrounding the use of high performance imaging gradient sets, where higher amplitude (T/m) and faster rate of change of gradient amplitude (slew rate in T/m/s) are almost always an advantage. Microscopy gradient capabilities range upwards to 10 T/m allowing high resolution and rapid imaging of small samples.

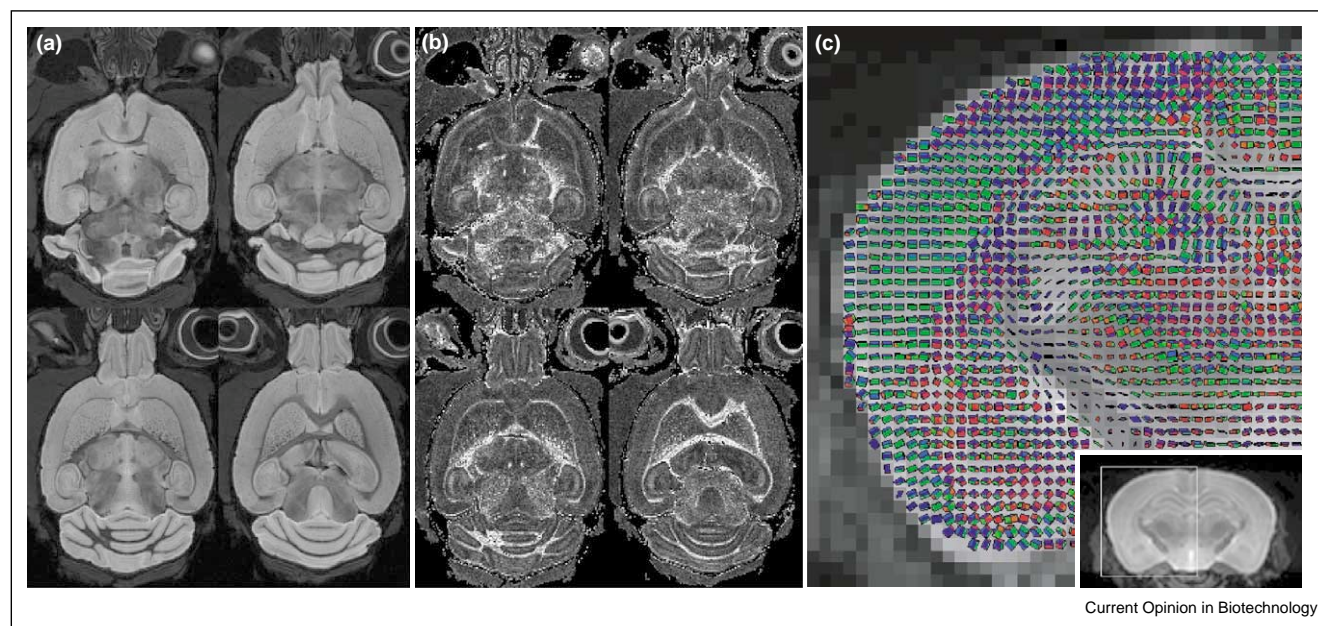
As experiments approach the theoretical limits of spatial resolution in MRM, the need for increasingly sensitive radiofrequency coils becomes apparent. Various groups have explored the use of microcoils (typically single or multiple turn solenoids with dimensions significantly smaller than 1 mm) to increase sensitivity in very small samples. Microcoils have been developed primarily for small sample NMR spectroscopy applications [3], but the highest resolution magnetic resonance images obtained have employed such designs [4,5,6].

Although this article is not an exhaustive review of the current MRM literature, it is intended to give the non-specialist reader a useful overview of current activity and key applications in this field. We have divided the review into sections covering what we consider to be the most significant areas of MRM research and development.

MRM of diffusion

MRM is capable of detecting and quantifying random molecular motion within tissues and the molecular interactions with restrictive or hindering boundaries. The popular diffusion tensor model of restricted diffusion (diffusion tensor imaging or DTI), although limited, provides a convenient and often acceptable image of the predominant structural directionality within a voxel (i.e. three-dimensional volume element) [7] (Figure 2). DTI has found application in studies of cerebral white matter tracts, where axonal bundles and fascicles provide a highly ordered and restrictive environment for water diffusion. High angular resolution diffusion (HARD) imaging techniques, such as diffusion spectrum imaging (DSI), have been proposed to address some of the limitations of DTI, particularly where axonal fibers cross within

Figure 2



Diffusion tensor microscopy of a fixed mouse brain at a nominal 75 μm isotropic resolution demonstrates the high signal-to-noise ratio and tissue contrast capabilities of volumetric MR histology. **(a)** Isotropic diffusion-weighted images of the mouse brain demonstrate basic anatomical organization. **(b)** Corresponding map of fractional anisotropy reveals regions of highly directional tissue organization chiefly in the white matter tracts of the brain. **(c)** Cuboids representing the diffusion tensor are overlaid on an anatomic reference image to visualize the complex tissue organization of the hippocampus, cortex and white matter tracts.

a voxel [8]. Taking its lead from human DTI and DSI studies, diffusion MRM has been applied to brain development in mice [9], dysmyelination models [10] and myocardial fiber structure [11].

Functional MRI

Functional MRI (fMRI) attempts to infer neuronal activity from changes in blood oxygenation level dependent (BOLD) contrast, cerebral blood flow or volume, or apparent diffusion coefficient. Of these approaches, BOLD dominates the fMRI literature in humans and has been studied extensively in rodents, particularly in rat models. In the past two years, as the neurophysiological basis of fMRI is explored, rodent fMRI experiments have become increasingly sophisticated [12–15]. In addition to studying the mechanisms of fMRI, we are seeing an increase in disease model [16,17], neural connectivity [18,19] and pharmaceutical studies [20–22] using fMRI as an imaging tool.

Tracing and tracking with MRM

Although MRM can exploit a wide variety of endogenous image contrasts (e.g. relaxation time, molecular diffusion and magnetic susceptibility), there is also great interest in developing exogenous contrast agents that target specific functions or structures within an organism. Despite its neurotoxicity, Mn^{2+} is now used at low concentrations as an axonal transport and trans-synaptic tracer [23,24,25•]

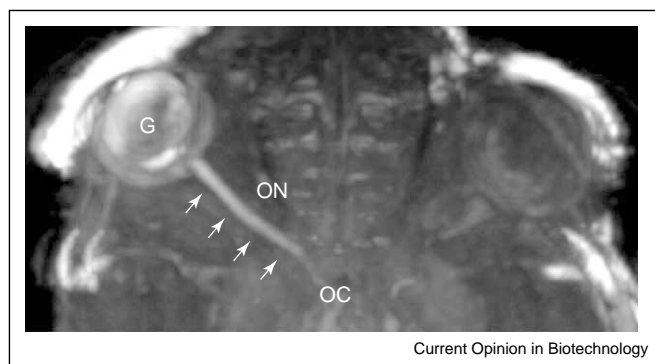
(Figure 3). Tracking the migration and distribution of appropriately labeled progenitor, stem or immune cells using MRM is also receiving considerable attention [26•,27]. Most MRM cell tracking has been developed using superparamagnetic iron oxide particles as T_2^* contrast labels [28•], although recent work suggests that T_1 agents such as Mn^{2+} might hold equal promise. The evolving field of molecular imaging is likely to contribute increasingly sensitive and specific T_1 and T_2^* contrast agents for MRM that target both gene expression and metabolism within a living organism.

MRM phenotyping and histology

MRM is well suited to anatomical phenotyping of genetically manipulated organisms such as transgenic mice [29–32]. The problem of increased throughput for MRM phenotyping of large numbers of rodents has received some attention, particularly from those groups employing low-field wide-bore clinical magnets. Recent work by Henkelman's group has demonstrated the practicality of simultaneous microscopy of multiple mice at lower magnetic field strengths [30]. Construction of MRM atlases of the brain for inbred mouse strains both in the developing embryo (see below) and adult animal are in progress at several sites [33,34].

In addition to *in vivo* imaging, *ex vivo* MRM histology allows higher resolution surveys of anatomy, particularly

Figure 3



In vivo manganese tracing of the mouse optic nerve (ON, arrows) from the globe of the eye (G) to the optic chiasm (OC), 24 h post-injection. Manganese is transported by the axonal microtubules and has been shown to traverse synapses allowing long-distance tract-tracing by MRM. (Image courtesy of Xiaowei Xiang, Caltech Biological Imaging Center).

in the central nervous system, than can be achieved *in vivo*, where total imaging time and physiological motion are factors [31,35]. Although MRM lacks the spatial resolution and staining flexibility of conventional optical histology, it preserves the three-dimensional structure of tissues and does not require tissue dehydration. Moreover, MRM imaging does not destroy the tissue and can therefore precede conventional histological analysis.

MRM in developmental biology

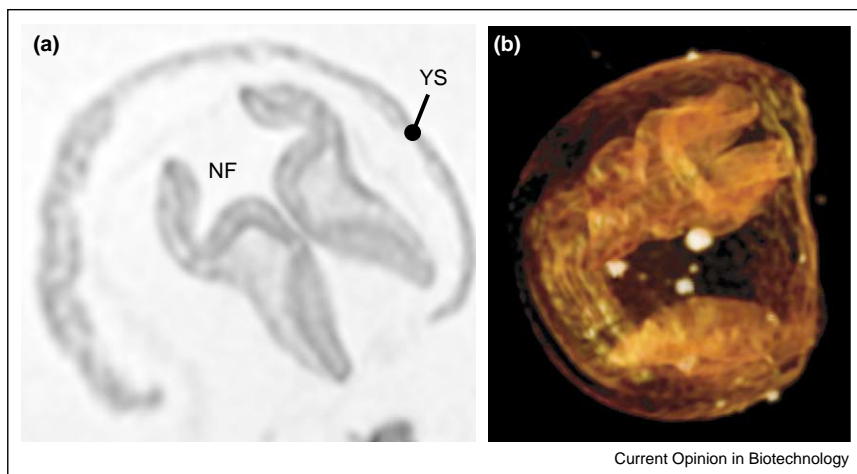
Another area in which MRM has proven effective is in the study of vertebrate development. MRM has been applied to the structural characterization of both the developing mouse [36,37] (Figure 4) and quail embryos and also to serial *in vivo* imaging of the *Xenopus laevis* embryo [38,39]. The *X. laevis* developmental model is a good match for

MRM, as the embryo is optically opaque owing to intracellular yolk inclusions, precluding non-invasive single- or multi-photon microscopy of internal embryonic development. High-resolution anatomical atlases of fixed mouse embryos at different stages of development are under construction by various groups [40,41].

MRM of disease models

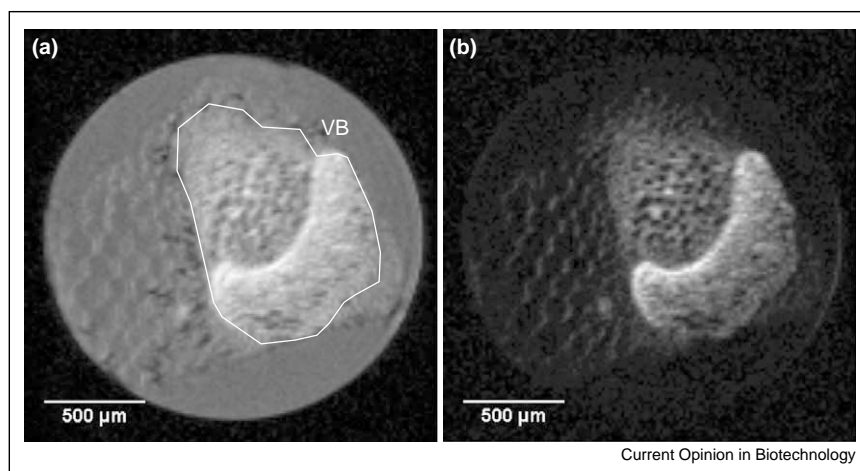
MRM is arguably better suited to serial, non-invasive imaging of animal disease models than are modalities employing ionizing radiation. One key application of serial MRM is monitoring the tumor response to therapy in rodent cancer models. MRM studies range from simple anatomical descriptions of tumor progression, such as total tumor volume [42], to sophisticated quantitation of vascular permeability [43], water diffusion [44] and

Figure 4



MRM of a fixed 8.5 dpc mouse embryo acquired at 11.7 Tesla. (a) Section through a three-dimensional MRM dataset demonstrating the neural folds (NF) and yolk sac (YS) of the developing embryo. (b) Volume rendering of the same dataset visualizes the intact embryo within the yolk sac. (Fixed embryo courtesy of Elizabeth Jones, Caltech Biological Imaging Center).

Figure 5



Diffusion-weighted MRM of a vascular bundle dissected from a celery stem and imaged at 11.7 Tesla. **(a)** Image without diffusion weighting shows the basic structure of the vascular bundle and surrounding tissue. **(b)** The same image in the presence of diffusion weighting highlights regions of low diffusivity (lower attenuation of water signal) in the vascular bundle (VB, highlighted).

blood oxygenation [45]. The perfusion and oxygenation of a tumor are considered to be important physiological parameters that affect the response to chemotherapeutic agents, and both BOLD and dynamic contrast enhanced MRM have been used for quantitative imaging of tumor models [45,46]. Other important animal models of human pathologies currently under investigation by MRM include Alzheimer's disease [47^{••}], epilepsy [48], Huntington's disease [49] and multiple sclerosis [10,50].

Vegetables and minerals: MRM outside the animal kingdom

Many of the strengths of MRM that make it ideal for imaging in animals also apply to non-invasive imaging of plants (Figure 5). Plants exhibit minimal physiological motion in the timescale of MRM, supporting higher spatial resolutions than can be achieved *in vivo* in animals [51,52]. MRM is especially suited to imaging flow and water distribution within plant samples [53].

MRM of non-biological samples is a mature field that, again, exploits the absence of physiological sample motion to obtain high spatial resolution images. The principle application areas include the study of water and oil in porous media [54], food science [55], the rheology of complex fluids [56] and the study of chemistry and mass transport in reactors [57,58]. MRM of water and oil within porous media, such as sedimentary rock, has important applications in geology [54]. MRM of porous media is not limited to liquids; successful studies of hyperpolarized Xe gas flow and diffusion in silica aerogels and zeolite particles have been reported [59^{••}]. MRM can generate images of flow and relaxation

changes within small biofilm reactors, which are otherwise unobtainable by conventional imaging techniques [58].

Conclusions

Applications of MRM are currently dominated by non-invasive structural imaging of biological systems both in living animals and for histology. Many other applications exist and the technique is arguably underexploited for non-biological imaging. MRM is clearly suited to opaque systems where optical microscopy is severely limited. MRM allows absolute volumetric mapping of mass transport phenomena, such as molecular diffusion and fluid flow, unobtainable by other imaging modalities. Spatial and temporal resolutions are limited by sensitivity, with typical minimum spatial resolutions in the order of tens of microns and imaging times ranging from minutes to hours.

What does the future hold for MRM? Advances in hardware performance might allow small improvements in routinely achieved spatial resolution, although it is unlikely that this will greatly exceed 40–50 μm in the mouse brain. Many of the advanced techniques applied in clinical MRI could find continued application and development in MRM, where the higher field-strength and altered relaxation properties of biological tissue require new solutions to imaging problems. Outside biology MRM still has room to grow, providing non-invasive volumetric imaging of fluid mechanics, rheology, reactor chemistry and mass transport. The advent of molecular imaging and targeted MRM contrast agents is particularly exciting with a wide range of new applications on the horizon.

Update

One of the more intriguing papers to be published in the last month describes the first practical demonstration of MRM [60] using the 'diffusion enhancement of signal and resolution' (DESIRE) effect first suggested by Lauterbur *et al.* in the early 1990s. Despite serious practical limitations, this paper demonstrated increases in the signal-to-noise of more than a factor of eight when compared to an equivalent conventional sequence. If borne out by further experiments, this sensitivity improvement could be of immense significance to studies at the limits of spatial resolution for MRM.

Acknowledgements

The authors would like to thank Xiaowei Zhang and Elizabeth Jones (both of the Caltech Biological Imaging Center) for providing the Mn²⁺ tract-tracing image and fixed 8.5 dpc mouse embryo, respectively. The authors are supported in part by the Beckman Institute and grants from the National Institute of Research Resources and the Human Brain Project (with contributions from the National Institute of Biomedical Imaging and Bioengineering and the National Institute of Mental Health).

References and recommended reading

Papers of particular interest, published within the annual period of review, have been highlighted as:

- of special interest
 - of outstanding interest
1. Haacke EM, Brown RW, Thompson MR, Venkatesan R: *Magnetic Resonance Imaging: Physical Principles and Sequence Design*. edn 1st. New York: John Wiley and Sons; 1999.
 2. Callaghan PT: *Principles of Nuclear Magnetic Resonance Microscopy*. Oxford: Oxford University Press; 1991.
 3. Ciobanu L, Jayawickrama DA, Zhang X, Webb AG, Sweedler JV: **Measuring reaction kinetics by using multiple microcoil NMR spectroscopy**. *Angew Chem Int Ed Engl* 2003, **42**:4669-4672.
 4. Lee SC, Kim K, Kim J, Lee S, Han Yi J, Kim SW, Ha KS, Cheong C: **One micrometer resolution NMR microscopy**. *J Magn Reson* 2001, **150**:207-213.
 5. Ciobanu L, Pennington CH: **3D micron-scale MRI of single biological cells**. *Solid State Nucl Magn Reson* 2004, **25**:138-141. Exciting demonstration of MRM with isotropic spatial resolution on the order of 3–4 microns using a 9 Tesla system.
 6. Grant SC, Buckley DL, Gibbs S, Webb AG, Blackband SJ: **MR microscopy of multicomponent diffusion in single neurons**. *Magn Reson Med* 2001, **46**:1107-1112.
 7. Pierpaoli C, Jezzard P, Basser PJ, Barnett A, DiChiro G: **Diffusion tensor MR imaging of the human brain**. *Radiology* 1996, **201**:637-648.
 8. Tuch DS, Reese TG, Wiegell MR, Wedeen VJ: **Diffusion MRI of complex neural architecture**. *Neuron* 2003, **40**:885-895.
 9. Zhang J, Richards LJ, Yarowsky P, Huang H, van Zijl PC, Mori S: **Three-dimensional anatomical characterization of the developing mouse brain by diffusion tensor microimaging**. *Neuroimage* 2003, **20**:1639-1648.
 10. Song SK, Sun SW, Ramsbottom MJ, Chang C, Russell J, Cross AH: **Dysmyelination revealed through MRI as increased radial (but unchanged axial) diffusion of water**. *Neuroimage* 2002, **17**:1429-1436.
 11. Jiang Y, Pandya K, Smithies O, Hsu EW: **Three-dimensional diffusion tensor microscopy of fixed mouse hearts**. *Magn Reson Med* 2004, **52**:453-460.
 12. Kannurpatti SS, Biswal BB: **Effect of anesthesia on CBF, MAP and fMRI-BOLD signal in response to apnea**. *Brain Res* 2004, **1011**:141-147.
 13. Austin VC, Blamire AM, Grieve SM, O'Neill MJ, Styles P, Matthews PM, Sibson NR: **Differences in the BOLD fMRI response to direct and indirect cortical stimulation in the rat**. *Magn Reson Med* 2003, **49**:838-847.
 14. Siegel AM, Culver JP, Mandeville JB, Boas DA: **Temporal comparison of functional brain imaging with diffuse optical tomography and fMRI during rat forepaw stimulation**. *Phys Med Biol* 2003, **48**:1391-1403.
 15. Kannurpatti SS, Biswal BB, Hudetz AG: **Baseline physiological state and the fMRI-BOLD signal response to apnea in anesthetized rats**. *NMR Biomed* 2003, **16**:261-268.
 16. Tenney JR, Duong TQ, King JA, Ferris CF: **fMRI of brain activation in a genetic rat model of absence seizures**. *Epilepsia* 2004, **45**:576-582.
 17. Tenney JR, Duong TQ, King JA, Ludwig R, Ferris CF: **Corticothalamic modulation during absence seizures in rats: a functional MRI assessment**. *Epilepsia* 2003, **44**:1133-1140.
 18. Keilholz SD, Silva AC, Raman M, Merkle H, Koretsky AP: **Functional MRI of the rodent somatosensory pathway using multislice echo planar imaging**. *Magn Reson Med* 2004, **52**:89-99.
 19. Shyu BC, Lin CY, Sun JJ, Chen SL, Chang C: **BOLD response to direct thalamic stimulation reveals a functional connection between the medial thalamus and the anterior cingulate cortex in the rat**. *Magn Reson Med* 2004, **52**:47-55.
 20. Shah YB, Prior MJ, Dixon AL, Morris PG, Marsden CA: **Detection of cannabinoid agonist evoked increase in BOLD contrast in rats using functional magnetic resonance imaging**. *Neuropharmacology* 2004, **46**:379-387.
 21. Xi ZX, Wu G, Stein EA, Li SJ: **Opiate tolerance by heroin self-administration: an fMRI study in rat**. *Magn Reson Med* 2004, **52**:108-114.
 22. Shoaib M, Lowe AS, Williams SC: **Imaging localised dynamic changes in the nucleus accumbens following nicotine withdrawal in rats**. *Neuroimage* 2004, **22**:847-854.
 23. Aoki I, Wu YJ, Silva AC, Lynch RM, Koretsky AP: **In vivo detection of neuroarchitecture in the rodent brain using manganese-enhanced MRI**. *Neuroimage* 2004, **22**:1046-1059.
 24. Pautler RG, Mongeau R, Jacobs RE: **In vivo trans-synaptic tract tracing from the murine striatum and amygdala utilizing manganese enhanced MRI (MEMRI)**. *Magn Reson Med* 2003, **50**:33-39.
 25. Pautler RG, Koretsky AP: **Tracing odor-induced activation in the olfactory bulbs of mice using manganese-enhanced magnetic resonance imaging**. *Neuroimage* 2002, **16**:441-448.
 - This is one of the key papers introducing manganese as a biologically relevant MRM contrast agent. Pautler and Koretsky still lead the field in this area.
 26. Shapiro EM, Skrtic S, Sharer K, Hill JM, Dunbar CE, Koretsky AP: **MRI detection of single particles for cellular imaging**. *Proc Natl Acad Sci USA* 2004, **101**:10901-10906.
 - This paper provides an essential proof-of-concept that MRM is capable of detecting single labeling particles for future cell tracking and location studies.
 27. Hinds KA, Hill JM, Shapiro EM, Laukkanen MO, Silva AC, Combs CA, Varney TR, Balaban RS, Koretsky AP, Dunbar CE: **Highly efficient endosomal labeling of progenitor and stem cells with large magnetic particles allows magnetic resonance imaging of single cells**. *Blood* 2003, **102**:867-872.
 28. Foster-Gareau P, Heyn C, Alejski A, Rutt BK: **Imaging single mammalian cells with a 1.5 T clinical MRI scanner**. *Magn Reson Med* 2003, **49**:968-971.
 - A short but significant paper correlating MR and fluorescence microscopy of cells from a human promonocytic cell line colabeled with superparamagnetic iron oxide and Dil. A custom gradient insert was added to a clinical scanner to achieve spatial resolution in the order of 100 micron.
 29. Lo C, Nabel E, Balaban R: **Meeting report: NHLBI symposium on phenotyping: mouse cardiovascular function and development**. *Physiol Genomics* 2003, **13**:185-186.
 30. Bock NA, Konyer NB, Henkelman RM: **Multiple-mouse MRI**. *Magn Reson Med* 2003, **49**:158-167.

31. Johnson GA, Cofer GP, Fubara B, Gewalt SL, Hedlund LW, Maronpot RR: **Magnetic resonance histology for morphologic phenotyping.** *J Magn Reson Imaging* 2002, **16**:423-429.
 32. Johnson GA, Cofer GP, Gewalt SL, Hedlund LW: **Morphologic phenotyping with MR microscopy: the visible mouse.** *Radiology* 2002, **222**:789-793.
 33. Kovacevic N, Henderson JT, Chan E, Lifshitz N, Bishop J, Evans AC, Henkelman RM, Chen XJ: **A three-dimensional MRI atlas of the mouse brain with estimates of the average and variability.** *Cereb Cortex* 2004, in press.
 34. Segars WP, Tsui BM, Frey EC, Johnson GA, Berr SS: **Development of a 4-D digital mouse phantom for molecular imaging research.** *Mol Imaging Biol* 2004, **6**:149-159.
 35. Johnson GA, Benveniste H, Black RD, Hedlund LW, Maronpot RR, Smith BR: **Histology by magnetic resonance microscopy.** *Magn Reson Q* 1993, **9**:1-30.
 36. Jacobs RE, Ahrens ET, Dickinson ME, Laidlaw D: **Towards a microMRI atlas of mouse development.** *Comput Med Imaging Graph* 1999, **23**:15-24.
 37. Chapon C, Franconi F, Roux J, Marescaux L, Le Jeune JJ, Lemaire L: **In utero time-course assessment of mouse embryo development using high resolution magnetic resonance imaging.** *Anat Embryol (Berl)* 2002, **206**:131-137.
 38. Papan C, Velan SS, Fraser SE, Jacobs RE: **3D time-lapse analysis of *Xenopus* gastrulation movements using mu MRI.** *Dev Biol* 2001, **235**:189.
 39. Jacobs RE, Papan C, Ruffins S, Tyszkla JM, Fraser SE: **MRI: volumetric imaging for vital imaging and atlas construction.** *Nat Rev Mol Cell Biol* 2003:SS10-SS16.
 40. Matsuda Y, Utsuzawa S, Kurimoto T, Haishi T, Yamazaki Y, Kose K, Anno I, Marutani M: **Super-parallel MR microscope.** *Magn Reson Med* 2003, **50**:183-189.
 41. Dhenain M, Ruffins SW, Jacobs RE: **Three-dimensional digital mouse atlas using high-resolution MRI.** *Dev Biol* 2001, **232**:458-470.
 42. Moats RA, Velan-Mullan S, Jacobs R, Gonzalez-Gomez I, Dubowitz DJ, Taga T, Khankaldyyan V, Schultz L, Fraser S, Nelson MD et al.: **Micro-MRI at 11.7 T of a murine brain tumor model using delayed contrast enhancement.** *Mol Imaging* 2003, **2**:150-158.
 43. Turetschek K, Roberts TP, Floyd E, Preda A, Novikov V, Shames DM, Carter WO, Brasch RC: **Tumor microvascular characterization using ultrasmall superparamagnetic iron oxide particles (USPIO) in an experimental breast cancer model.** *J Magn Reson Imaging* 2001, **13**:882-888.
 44. Carano RA, Ross AL, Ross J, Williams SP, Koeppen H, Schwall RH, Van Bruggen N: **Quantification of tumor tissue populations by multispectral analysis.** *Magn Reson Med* 2004, **51**:542-551.
 45. Robinson SP, Rijken PF, Howe FA, McSheehy PM, van der Sanden BP, Heerschap A, Stubbs M, van der Kogel AJ, Griffiths JR: **Tumor vascular architecture and function evaluated by non-invasive susceptibility MRI methods and immunohistochemistry.** *J Magn Reson Imaging* 2003, **17**:445-454.
 46. Jiang L, Zhao D, Constantinescu A, Mason RP: **Comparison of BOLD contrast and Gd-DTPA dynamic contrast-enhanced imaging in rat prostate tumor.** *Magn Reson Med* 2004, **51**:953-960.
 47. Zhang J, Yarowsky P, Gordon MN, Di Carlo G, Munireddy S, van Zijl PC, Mori S: **Detection of amyloid plaques in mouse models of Alzheimer's disease by magnetic resonance imaging.** *Magn Reson Med* 2004, **51**:452-457.
- This is an important example of combining transgenic mouse models with MRM, to demonstrate detection limits for amyloid plaques, a long-standing question in both MRI and MRM.
48. Wolf OT, Dyakin V, Patel A, Vadasz C, de Leon MJ, McEwen BS, Bulloch K: **Volumetric structural magnetic resonance imaging (MRI) of the rat hippocampus following kainic acid (KA) treatment.** *Brain Res* 2002, **934**:87-96.
 49. Guzman R, Meyer M, Lovblad KO, Ozdoba C, Schroth G, Seiler RW, Widmer HR: **Striatal grafts in a rat model of Huntington's disease: time course comparison of MRI and histology.** *Exp Neurol* 1999, **156**:180-190.
 50. Ahrens ET, Laidlaw DH, Readhead C, Brosnan CF, Fraser SE, Jacobs RE: **MR microscopy of transgenic mice that spontaneously acquire experimental allergic encephalomyelitis.** *Magn Reson Med* 1998, **40**:119-132.
 51. Kockenberger W, De Panfilis C, Santoro D, Dahiya P, Rawsthorne S: **High resolution NMR microscopy of plants and fungi.** *J Microsc* 2004, **214**:182-189.
 52. Kockenberger W: **Nuclear magnetic resonance micro-imaging in the investigation of plant cell metabolism.** *J Exp Bot* 2001, **52**:641-652.
 53. Kuchenbrod E, Kahler E, Thurmer F, Deichmann R, Zimmermann U, Haase A: **Functional magnetic resonance imaging in intact plants — quantitative observation of flow in plant vessels.** *Magn Reson Imaging* 1998, **16**:331-338.
 54. Kossel E, Weber M, Kimmich R: **Visualization of transport: NMR microscopy experiments with model objects for porous media with pore sizes down to 50 μ m.** *Solid State Nucl Magn Reson* 2004, **25**:28-34.
 55. Bonny JM, Rouille J, Della Valle G, Devaux MF, Douliez JP, Renou JP: **Dynamic magnetic resonance microscopy of flour dough fermentation.** *Magn Reson Imaging* 2004, **22**:395-401.
 56. Xia Y, Callaghan PT: **Imaging the velocity profiles in tubeless siphon flow by NMR microscopy.** *J Magn Reson* 2003, **164**:365-368.
 57. Seymour JD, Codd SL, Gjersing EL, Stewart PS: **Magnetic resonance microscopy of biofilm structure and impact on transport in a capillary bioreactor.** *J Magn Reson* 2004, **167**:322-327.
 58. Manz B, Volke F, Goll D, Horn H: **Measuring local flow velocities and biofilm structure in biofilm systems with magnetic resonance imaging (MRI).** *Biotechnol Bioeng* 2003, **84**:424-432.
 59. Kaiser LG, Meersmann T, Logan JW, Pines A: **Visualization of gas flow and diffusion in porous media.** *Proc Natl Acad Sci USA* 2000, **97**:2414-2418.
- This is a wonderful demonstration of MRM employing laser-polarized ^{129}Xe instead of the more typical ^1H species. It provides ample proof that mass transport of gases in porous media can be quantified using magnetic resonance.
60. Ciobanu L, Webb AG, Pennington CH: **Signal enhancement by diffusion: experimental observation of the "DESIRE" effect.** *J Magn Reson USA* 2004, **170**:252-256.